

Analysis of cutting forces and roughness during hard turning of bearing steel

Abderrahim Bouziane*¹, Lakhdar Boulanouar¹, Mohamed Walid Azizi^{1,2},
Ouahid Kebblouti¹ and Salim Belhadi^{1,3}

¹Advanced Technologies in Mechanical Production Research Laboratory (LRTAPM), Badji Mokhtar - Annaba University, P.O. Box 12, 23000 Annaba, Algeria

²Technical Science Department, Abdelhafid Boussouf-Mila University Center, 43000, Algeria

³Mechanics and Structures Research Laboratory (LMS), May 8th 1945 University, P.O. Box 401, Guelma 24000, Algeria

(Received September 12, 2017, Revised January 4, 2018, Accepted February 7, 2018)

Abstract. An experimental study has been carried out to analyze the effect of cutting parameters (cutting speed, feed and depth of cut) and tool nose radius on the surface roughness and the cutting force components during hard turning of the AISI 52100 (50 HRC) steel with a ceramic cutting tool. The tests have been conducted according to the methodology of planning experiments, based on an orthogonal plan of Taguchi (L27). By using the response surface methodology (RSM), the components of the cutting force and the roughness of the machined surface were modeled and the effects of the input parameters were analyzed statistically by ANOVA and RSM. The results show that the feed (f), the tool nose radius (r), the cutting speed (V_c), the interaction between feed and tool nose radius ($f \times r$) as well as that of the quadratic effect (f^2) all have significant effects on the surface roughness (R_a). The feed is the most influencing factor with a contribution of 47.31%. The components of the cutting force were strongly influenced by the depth of cut, followed by the advance with a lower degree. By comparing the experimental values with those predicted by the models of the cutting force components and the surface roughness, it appears that they are in very good correlation.

Keywords: hard turning; AISI 52100; cutting force; roughness; ANOVA; mixed ceramic

1. Introduction

Developments in cutting tools and machine tools in the last few decades have made it possible to cut materials in their hardened state. The advantages of producing components in hardened state can be listed as (Azizi *et al.* 2012, Bouacha *et al.* 2014, Kebblouti *et al.* 2017): reduction of machining costs, reduction of lead-time, reduction of number of necessary machine tools, improved surface integrity, reduction of finishing operations and elimination of part distortion caused by heat treatment.

The Al₂O₃-based ceramics have been widely used in the machining of hardened steel due to their high hardness, wear resistance and heat resistance (Kumar *et al.* 2003, Xiaobin *et al.* 2016, Yin *et al.* 2015). On the other hand, Al₂O₃ based tools have a high degree of brittleness, which usually leads to a short, tool life due to excessive chipping or fracture especially when machining hardened materials. In order to improve toughness, Al₂O₃ based ceramic cutting tools are usually reinforced with TiC, TiN, ZrO₂ and TiB₂ additions. These additions result in some improvement, but the toughness of Al₂O₃ based tools are still much less than that of other tools such as cemented carbides. As a result, the possibility of sudden failures when machining hardened materials with Al₂O₃ based ceramics is very high (Hessainia

et al. 2013a).

Several researchers have made attempts to optimize and understand the effect of various machining parameters for the control of the finish hard turning process. Das *et al.* (2017), Rashid *et al.* (2016), Aouici *et al.* (2014), Bouzid *et al.* (2014), Shihab *et al.* (2014) and Gunay *et al.* (2013) conducted the experiments on hard turning of various grades of steels using different kinds of tools and identified different factors affecting surface roughness, tool wear, cutting force and power consumption, etc.

Neşeli *et al.* (2011) focused on the influence of tool geometry on the surface finish obtained in turning of AISI 1040 steel with Al₂O₃/TiC tool. Their study focused on the effect of tool geometry parameters on the surface roughness during turning. The response surface methodology and a prediction model were developed related to the Ra using experimental data. The results indicated that the tool nose radius was the dominant factor on the surface roughness with 51.45% contribution in the total variability of model. Hessainia *et al.* (2013b) focused on developing an empirical model for the prediction of surface roughness using linear regression analysis with logarithmic data transformation in finish turning. Also, they investigated the impact of cutting speed, depth of cut, feed rate, tool nose radius and tool vibration on the surface roughness. Ozel and Karpuz *et al.* (2005) have found that cutting parameters (feed, cutting speed, depth of cut, tool geometry and material properties of tool) directly influence the surface finish of machined components. However, among the

*Corresponding author, Ph.D.
E-mail: rahim_bou23@yahoo.fr

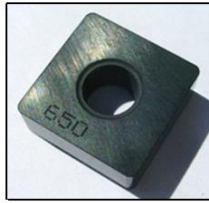


Fig. 1 Mixed ceramic insert (CC650)

cutting force, thrust force, and feed force, the former prominently influences power consumption and this work considers only cutting force as one of the endogenous factors. In their experimental research work, Meddour *et al.* (2015) indicated that the best surface roughness is obtained with the combination of lowest feed rate and largest nose radius as well as the opposite is true. Chou and Song *et al.* (2004) have investigated the effect of tool nose radius on hardened steel (AISI 52100) in hard turning, the better surface finish was obtained in larger tool nose radius.

Aouici *et al.* (2014) studied the effects of feed rate, cutting speed and depth of cut on surface roughness, tangential force, specific cutting force and power in hard turning of AISI D3 hardened steel using ceramic cutting tool. They found that the feed rate is the most influencing factor on surface roughness. They recommended to machine with higher cutting speed, lower depth of cut and feed rate ranged from 0.12 to 0.13 mm/rev to ensure better surface roughness and minimum cutting forces. Bensouilah *et al.* (2016) showed that the surface quality obtained with the coated CC6050 ceramic insert is 1.6 times better than the one obtained with uncoated CC650 ceramic insert. However, the uncoated ceramic insert was useful in reducing the machining force. Bouacha *et al.* (2010) experimentally investigated the impact of machining parameters (i.e., cutting speed, feed rate and depth of cut) on the cutting forces and surface roughness during hard turning of AISI 52100 bearing steel (64 HRC) with CBN tool using RSM. Results showed that depth of cut exhibited the most significant role on the cutting force components and surface roughness is largely influenced by feed rate.

In an earlier investigation, Asina *et al.* (2007) employed the Taguchi technique and ANOVA in order to optimize surface roughness for mixed ceramic ($\text{Al}_2\text{O}_3+\text{TiC}$) tools. To model the machining properties as function of hard turning process parameters, many researchers have used Response Surface Methodology (RSM) (Neşeli *et al.* 2011, Paiva *et al.* 2009, Paiva *et al.* 2012). In this methodology, the effect of cutting parameters on machining outputs are obtained using a set of experiments capable of generate an appropriate dataset for efficient statistical analysis, which in turn produces valid and objective models. These models can be used in optimization, simulation or prediction of turning process behavior, mainly within the experimental range (Paiva *et al.* 2012).

The aim of this work is to study the effects of cutting conditions (cutting speed, depth of cut, feed and nose radius tool) on cutting forces and surface roughness during finish hard turning of AISI 52100 steel with coated $\text{Al}_2\text{O}_3 + \text{TiC}$ mixed ceramic cutting tools. In this work, only significant parameters will be used to develop mathematical models

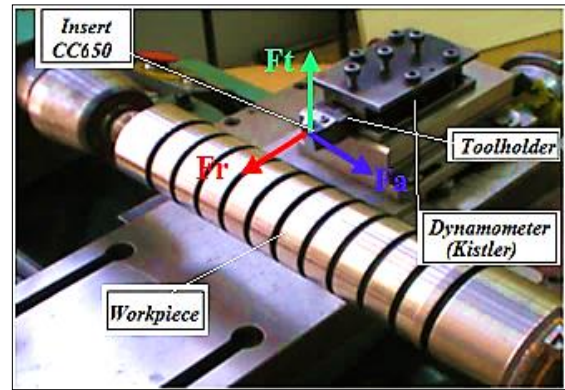


Fig. 2 Experimental setup to measure cutting forces

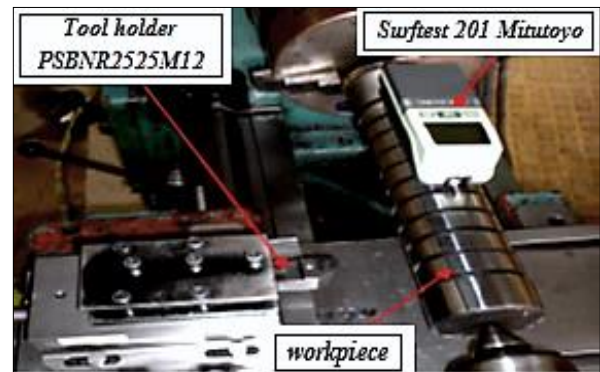


Fig. 3 Experimental setup to measure roughness

using the Response Surface Method (RSM). The latter is a collection of mathematical and statistical techniques which are useful for the modeling and analysis of problems in which the response of interest is influenced by several variables and the objective is to optimize the response.

2. Experimental procedure

The machining operations relating to the cutting forces tests were carried out on round samples of AISI grade 52100 treated steel, 63 mm in diameter and 450 mm in length. Due to its high wear resistance, the AISI 52100 steel is recommended especially for the production of balls, rollers, rings and bearing cages. It is also used as cold forming dies, rolling mill rolls and wear coatings (Yaltese *et al.* 2009). Its chemical composition is given as follows: 0.95%C; 0.41% Mn; 0.28% Si; 0.018%P; 0.018% S; 0.12% Cu; 1.50% Cr; 0.08% Ni; 0.011% Mo; 0.014% Co. A TOS TRENCIN lathe, model SN40, spindle power output of 6.6 kW has been used for machining operations. The cutting tool used are mixed ceramic inserts is shown in Figs. (1) and (2). All information relating to the cutting inserts is given in Table 1. The tool holder is designated PSBNR2525M12 with a geometry of the active part materialized by the following angles: $\chi_r = 75^\circ$; $\alpha = 6^\circ$; $\gamma = -6^\circ$ and $\lambda = -6^\circ$. Characterization of the workpiece surface topography is made with a portable roughness tester Mitutoyo, with the following characteristics: Resolution: $0.1 \mu\text{m}$, Filter used: 0.8, used feed: 2.5×5 . The measurement

Table 1 Information on the plates used

Cutting material	Grade	ISO Designation	Radius of nose	Mark	Composition
Mixed ceramic	CC650	SNGA120408T01020	0.8	Sandvik	70% Al ₂ O ₃ + 30% TiC
		SNGA120412T01020	1.2		
		SNGA120416T01020	1.6		

Table 2 The variation levels of cutting parameters

Level	<i>V_c</i> (m/min)	<i>f</i> (mm/rev)	<i>ap</i> (mm)	<i>r</i> (mm)
L 1	95	0.08	0.15	0.8
L 2	140	0.12	0.30	1.2
L 3	185	0.16	0.45	1.6

Table 3 Conditions and results of the AISI 52100 steel heat treatment

Steel	Hardness before treatment	Heat treatment			Average hardness after treatment
		Austenization	Quenching	Tempering	
AISI 52100	28 HRC	Maintaining at 840°C	Cooling fast/Oil tray	380°C	50HRC

of the roughness is carried out directly on the same machine and without disassembling the part as shown in Fig. 3. The cutting forces were measured in real time with a Kistler three component dynamometer model 9257 B linked via a multichannel charge amplifier (type 5011 B) to high impedance cable. The cutting tests were carried out without lubrication and under the cutting conditions indicated in Table 2. In order to increase the hardness of the samples up to 50 HRC, a hardening process followed by a tempering have been performed, (Table 3).

3. Planning of experiments

The planning of the experiments plays a very important role in carrying out the experiments with the available resource. The orthogonal table was chosen because of the minimum number of experimental tests required which is more efficient in handling the large number of variable factors than traditional factorial planning. In addition, the orthogonal table allows determining the contribution of each factor that influences the quality. This experiment indicates four main machining parameters, cutting speed (*V_c*), feed (*f*), depth of cut (*ap*) and radius of tool nose (*r*). All degrees of freedom were calculated by considering only the main effects of the factors; their interactions are excluded in the data analysis. Therefore, the degree of freedom (*DF*) for this experiment is calculated according to Eq. (1)

$$DF = (\text{number levels} - 1) \times (\text{number of factors}) \quad (1)$$

$$DF = (3 - 1) \times 4; DF = 8$$

According to the Taguchi method, all the *DF* of the orthogonal table chosen must be greater than or equal to all the *DF* required for the experiments. Thus, Table L₂₇ was chosen to increase the accuracy of the experiment (Montgomery 2001). The experiments were carried out based on the orthogonal table L₂₇. The cutting parameters (*V_c*, *f*, *ap* and *r*) and the studied technological parameters

Table 4 Experimental plan and results

N°	Factors				Roughness	Cutting forces		
	<i>V_c</i>	<i>f</i>	<i>ap</i>	<i>r</i>	<i>Ra</i>	<i>Fa</i>	<i>Fr</i>	<i>Ft</i>
1	95	0.08	0.15	0.8	0.44	23.2	57	50.3
2	95	0.08	0.3	1.2	0.34	45.8	106	92.9
3	95	0.08	0.45	1.6	0.24	68.5	173	145
4	95	0.12	0.15	1.2	0.55	23.6	84.2	71
5	95	0.12	0.3	1.6	0.43	63.6	165	128
6	95	0.12	0.45	0.8	0.69	88	190	141
7	95	0.16	0.15	1.6	0.66	23.9	111	85
8	95	0.16	0.3	0.8	1.13	59.5	160	117
9	95	0.16	0.45	1.2	0.98	90.3	215	163
10	140	0.08	0.15	1.2	0.32	20.9	65.5	55.8
11	140	0.08	0.3	1.6	0.23	42.1	119	104
12	140	0.08	0.45	0.8	0.35	83.6	160	131
13	140	0.12	0.15	1.6	0.38	21.6	86.4	73
14	140	0.12	0.3	0.8	0.68	47.3	140	115
15	140	0.12	0.45	1.2	0.45	85.5	199	161
16	140	0.16	0.15	0.8	1.04	41.8	99.6	78
17	140	0.16	0.3	1.2	0.76	66.7	19	127
18	140	0.16	0.45	1.6	0.56	87.1	233	177
19	185	0.08	0.15	1.6	0.19	19.7	77	60.5
20	185	0.08	0.3	0.8	0.34	57.9	116	98
21	185	0.08	0.45	1.2	0.28	79.9	163	136
22	185	0.12	0.15	0.8	0.63	37.6	90.8	68
23	185	0.12	0.3	1.2	0.53	61.4	145	123
24	185	0.12	0.45	1.6	0.31	80.8	207	160
25	185	0.16	0.15	1.2	0.81	38.3	101	83
26	185	0.16	0.3	1.6	0.58	68	174	131
27	185	0.16	0.45	0.8	1.03	47.2	133	98

Ra (μm), *Fa* (N), *Fr* (N) and *Ft* (N) are shown in table 4. The observed values of the surface roughness and cutting forces were used to determine the significant factors on machining performance. The observed values of the surface roughness and cutting forces have been used to identify the significant factors and interactions. The empirical models are developed in order to determine the correlation between the input parameters and the technological parameters studied (responses): Surface roughness and the cutting force components.

In addition, the response areas of the relevant factors corresponding to each (ANOVA) analysis were presented. These response surfaces provide an analysis of the most significant factors related to surface roughness and cutting forces during the hard turning of the rolling steel with the mixed ceramic tool (CC650).

4. Results interpretation

4.1 Sensitivity of the surface roughness as a function of *V_c*, *f*, *ap* and *r*

Table 5 Analysis of variance (ANOVA) for Ra

Source	SC sq	DF	MS	F-Value	Prob> F	Cont. %	Remark
Model	1.85000	14	0.13000	80.3800	< 0.0001	–	Signif.
A-Vc	0.02100	1	0.02100	12.9000	0.00370	1.1290	Signif.
B-f	0.88000	1	0.88000	536.900	< 0.0001	47.3118	Signif.
C-ap	0.00000	1	0.00000	0.00000	1.00000	0.0000	No Signif.
D-r	0.29000	1	0.29000	178.270	< 0.0001	15.5914	Signif.
Vc x f	0.00005	1	0.00005	0.03300	0.85800	0.00300	No Signif.
Vc x ap	0.00001	1	0.00001	0.00564	0.94100	0.00050	No Signif.
Vc x r	0.00014	1	0.00014	0.08300	0.77800	0.00740	No Signif.
f x ap	0.00054	1	0.00054	0.33000	0.57550	0.02920	No Signif.
f x r	0.01500	1	0.01500	9.08000	0.01080	0.80650	Signif.
ap x r	0.00016	1	0.00016	0.09700	0.76110	0.00850	No Signif.
Vc ²	0.00562	1	0.00562	3.43000	0.08880	0.30220	No Signif.
f ²	0.01300	1	0.01300	8.09000	0.01480	0.69890	Signif.
ap ²	0.00008	1	0.00008	0.04800	0.83100	0.00420	No Signif.
r ²	0.00008	1	0.00008	0.04800	0.83110	0.00420	No Signif.
Residual	0.02000	12	0.00164	–	–	–	–
Cor Total	1.86000	26	–	–	–	100	–

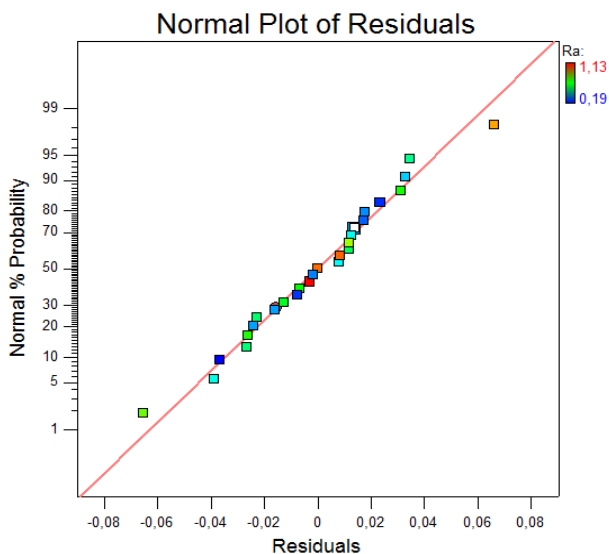


Fig. 4 Normal probabilities of surface roughness

The results of variance analysis (ANOVA) for surface roughness (Ra) are shown in Table 5. The analysis is carried out for a significance level $\alpha = 0.5$, (i.e., for a confidence level of 95%). In this table, the degrees of freedom (DF), sum of squares (SC sq), mean square (MS), F-value and probabilities, in addition to the contribution (Cont. %) of each factor, are also shown. The analysis of the results shows that the feed (f), the tool nose radius (r), the cutting speed (Vc), the interaction between the feed and tool nose radius ($f \times r$) and the quadratic effect f^2 all have significant effects on the surface roughness (Ra). The feed is the most influential factor with a contribution of 47.31%.

The normal probability graph of residuals of the surface roughness shown in Fig.4 shows that the residuals are very close to the straight line of normality, which proves that the



Fig. 5 Comparison of the measured and estimated surface roughness (Ra)

limits mentioned in the first degree model are the only significant factors (Montgomery 2001). In addition to the normality that seems acceptable, the correlation coefficients are very high.

4.2 Regression analysis for Ra as a function of Vc, f, ap and r

The regression equations are generated by Design-Expert Software. The linear models multiple regression have been developed for the surface roughness (Ra) as a function of the cutting parameters (cutting speed, feed, depth of cut and the radius of the tool nose). Consequently, the equation of the prediction model of the surface roughness (Ra) as a function of the main factors and their statistically significant interactions is as follows

$$Ra = +0.32519 - 0.0047Vc + 4.4963f + 0.3386r - 4.7916f \cdot r + 34.0277f^2 \quad (2)$$

The value of the determination coefficient R^2 for the model of the surface roughness (Ra) is equal to 0.9894. This means that this model explains 98.94% of changes in surface roughness level and consequently 1.06% remains unexplained. The surface roughness of the adjusted coefficient value of the model determination is $AdjR^2 = 97.71\%$. It represents a correction of the R^2 , which makes it possible to take into account the number of variables used in the model. These two coefficients show a very good correlation between the values predicted by this model and the results obtained experimentally. Fig. 5 shows a comparison of the values estimated by the model deduced from the roughness and the values measured experimentally.

4.3 Analysis of the evolution of the cutting forces according to Vc, f, ap and r

Table 6 shows the ANOVA analysis results so that the influence of different factors on the axial force (Fa) can be determined. The results analysis shows that the depth of cut affects the axial force enormously with a contribution of 25.98%. The second factor that has the greatest influence on

Table 6 Analysis of variance (ANOVA) for F_a

Source	SC sq	DF	MS	F-Value	Prob> F	Cont. %	Remark
Model	14216.39	14	1015.46	28.61	< 0.0001	–	Signif.
V_c	185.77	1	185.77	5.23	0.0411	1.2687	Signif.
f	643.88	1	643.88	18.14	0.0011	4.3974	Signif.
ap	3804.83	1	3804.83	107.18	< 0.0001	25.9851	Signif.
r	156.7	1	156.7	4.41	0.0574	1.0702	Signif.
$V_c \times f$	258.72	1	258.72	7.29	0.0193	1.7669	Signif.
$V_c \times ap$	569.24	1	569.24	16.04	0.0017	3.8876	Signif.
$V_c \times r$	244.07	1	244.07	6.88	0.0223	1.6669	Signif.
$f \times ap$	296.19	1	296.19	8.34	0.0136	2.0228	Signif.
$f \times r$	581.04	1	581.04	16.37	0.0016	3.9682	Signif.
$ap \times r$	376.13	1	376.13	10.6	0.0069	2.5688	Signif.
V_c^2	4.74	1	4.74	0.13	0.7211	0.0324	No Signif.
f^2	54.8	1	54.8	1.54	0.2378	0.3743	No Signif.
ap^2	73.73	1	73.73	2.08	0.1751	0.5035	No Signif.
r^2	74.44	1	74.44	2.1	0.1732	0.5084	No Signif.
Residual	425.98	12	35.5	–	–	2.9092	–
Cor Total	14642.37	26	–	–	–	100	–

Table 7 Analysis of variance (ANOVA) for F_r

Source	SC sq	DF	MS	F-Value	Prob> F	Cont.%	Remark
Model	60381.21	14	4312.94	142.41	< 0.0001	–	Signif.
V_c	51.89	1	51.89	1.71	0.2151	0.0854	No Signif.
f	6204.64	1	6204.64	204.87	< 0.0001	10.214	Signif.
ap	15080.06	1	15080.06	497.92	< 0.0001	24.825	Signif.
r	368.77	1	368.77	12.18	0.0045	0.6071	Signif.
$V_c \times f$	1372.27	1	1372.27	45.31	< 0.0001	2.2591	Signif.
$V_c \times ap$	1151.66	1	1151.66	38.03	< 0.0001	1.8959	Signif.
$V_c \times r$	604.63	1	604.63	19.96	0.0008	0.9954	Signif.
$f \times ap$	188.29	1	188.29	6.22	0.0283	0.3100	Signif.
$f \times r$	1111.04	1	1111.04	36.68	< 0.0001	1.8290	Signif.
$ap \times r$	1447.83	1	1447.83	47.8	< 0.0001	2.3835	Signif.
V_c^2	105.56	1	105.56	3.49	0.0865	0.1738	No Signif.
f^2	621.52	1	621.52	20.52	0.0007	1.0232	Signif.
ap^2	370.78	1	370.78	12.24	0.0044	0.6104	Signif.
r^2	0.31	1	0.31	0.01	0.9209	0.0005	No Signif.
Residual	363.44	12	30.29	–	–	0.5983	–
Cor Total	60744.64	26	–	–	–	100	–

the axial force (F_a) is the advance per revolution (f), its contribution is 4.39%. The cutting speed (V_c) and the radius of the tool noze (r) are characterized by contributions of 1.26% et 1.07%, respectively. The interactions ($(V_c \times f)$, $(V_c \times ap)$, $(V_c \times r)$, $(f \times ap)$, $(f \times r)$, $(ap \times r)$) have significant effects on the axial force (F_a).

The ANOVA results for the radial force (F_r) are given in Table 7. In this case, the depth of cut (ap) is the most significant factor with a contribution of 24.82%, followed by the advance (f) with a contribution of 10.21%. The interactions between the depth of cut and the radius of tool

Table 8 Analysis of variance (ANOVA) for F_t

Source	SC sq	DF	MS	F-Value	Prob> F	Cont. %	Remark
Model	33445.74	14	2388.98	186.87	< 0.0001	–	Signif.
V_c	27.7	1	27.7	2.17	0.1668	0.0824	No Signif.
f	2206.04	1	2206.04	172.56	< 0.0001	6.5658	Signif.
ap	9398.21	1	9398.21	735.13	< 0.0001	27.9716	Signif.
r	276.68	1	276.68	21.64	0.0006	0.8235	Signif.
$V_c \times f$	594.05	1	594.05	46.47	< 0.0001	1.7681	Signif.
$V_c \times ap$	535.96	1	535.96	41.92	< 0.0001	1.5952	Signif.
$V_c \times r$	232.56	1	232.56	18.19	0.0011	0.6922	Signif.
$f \times ap$	351.12	1	351.12	27.46	0.0002	1.0450	Signif.
$f \times r$	639.96	1	639.96	50.06	< 0.0001	1.9047	Signif.
$ap \times r$	973.01	1	973.01	76.11	< 0.0001	2.8959	Signif.
V_c^2	159.82	1	159.82	12.5	0.0041	0.4757	Signif.
f^2	402.89	1	402.89	31.51	0.0001	1.1991	Signif.
ap^2	338.5	1	338.5	26.48	0.0002	1.0075	Signif.
r^2	79.69	1	79.69	6.23	0.0281	0.2372	Signif.
Residual	153.41	12	12.78	–	–	0.4566	–
Cor Total	33599.16	26	–	–	–	100	–

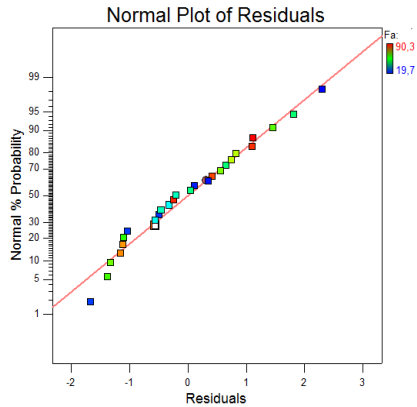
noze ($ap \times r$), cutting speed and feed rate ($V_c \times f$) with contributions of 2.38% et 2.25% respectively. The interactions between the cutting speed and the depth of cut ($V_c \times ap$), the feed and the tool noze radius ($f \times r$) and the quadratic effect (f^2) with contributions of 1.89%, 1.82% and 1.02% respectively. The quadratic effect (ap^2) and the interactions ($V_c \times r$) and ($f \times ap$) all have a significant effect on the radial force (F_r).

Table 8 shows the ANOVA results on tangential force (F_t). It can be seen that the depth of cut (ap) is the most important factor affecting the tangential force. Its contribution is 27.97%. The second factor that has the greatest influence on the tangential force (F_t) is the advance per revolution (f), its contribution is 6.56%, the tool nose radius (r) contributes only 0.82%. The interactions ($(V_c \times f)$, $(V_c \times ap)$, $(V_c \times r)$, $(f \times ap)$, $(f \times r)$, $(ap \times r)$) and quadratic effect (V_c^2 , f^2 , ap^2 , r^2) all have a significant effect on the tangential force (F_t).

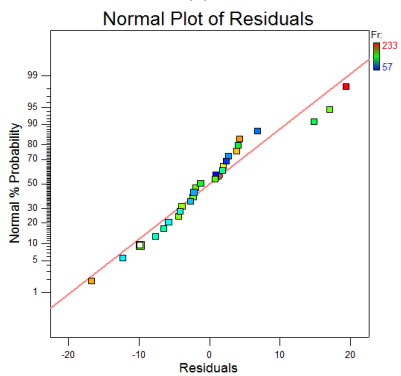
The graphs of normal probabilities of residual axial force (F_a), radial force (F_r) and tangential force (F_t) are respectively illustrated in Figs 6 (a), (b) and (c). They indicate that the residues are very close to the normal line of normality, which means that the limits mentioned in the first degree model are the only significant factors. Therefore, normality seems acceptable and the correlation coefficients are very high, indicating that the experimental results are in good agreement with the values predicted by the model.

4.4 Regression analysis of cutting forces as a function of V_c , f , ap and r

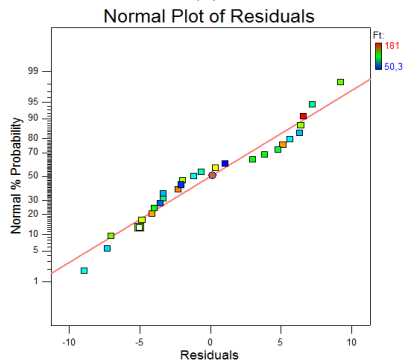
The hard turning forces depend on several factors such as depth of cut (ap), feed (f), cutting speed (V_c), geometry of the cutting tool, etc. In this work, the modeling of the



(a)



(b)



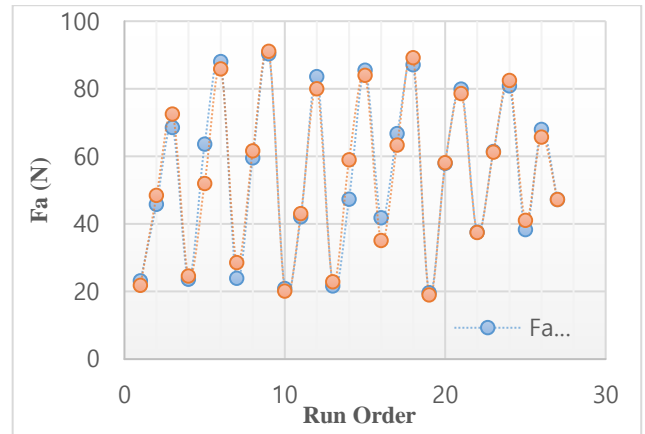
(c)

Fig. 6 Normal probability of cutting forces residues (a): F_a , (b): F_r et (c): F_t

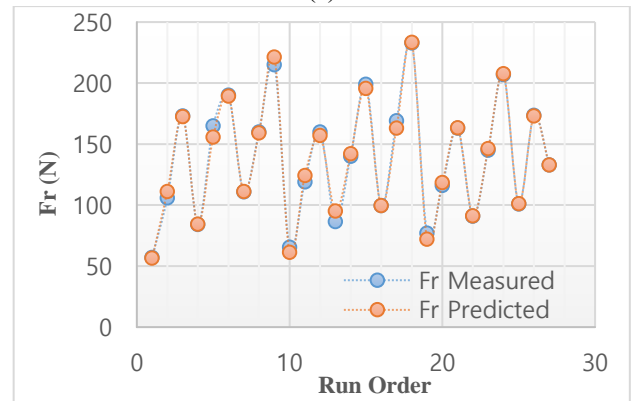
cutting forces by the multiple nonlinear regression shows the influence of the four main machining parameters that are: cutting speed, feed, depth of cut, tool nose radius and their interactions. Consequently, the equations of the models adapted in terms of real factors for the cutting forces are given below.

$$F_a = -60.25 + 0.45 V_c + 656.65 f + 398.48 ap - 67.70 r - 2.66 V_c \cdot f - 1.05 V_c \cdot ap + 0.26 V_c \cdot r - 855.19 f \cdot ap + 449.17 f \cdot r + 96.37 ap \cdot r \quad (3)$$

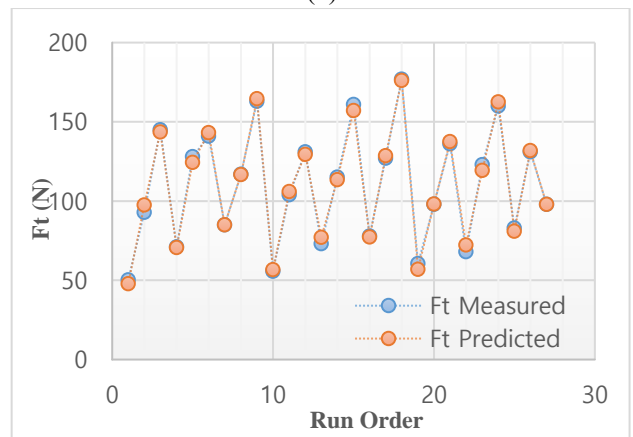
$$F_r = -160.31 + 2342.96 f + 607.93 ap - 157.29 r - 6.14 V_c \cdot f - 1.50 V_c \cdot ap + 0.41 V_c \cdot r - 681.85 f \cdot ap + 621.11 f \cdot r + 189.07 ap \cdot r - 6361.11 f^2 - 349.38 ap^2 \quad (4)$$



(a)



(b)



(c)

Fig. 7 Comparison of the measured and estimated values of the cutting force components (a): F_a , (b): F_r and (c): F_t

$$F_t = -167.28 + 1765.66 f + 523.78 ap - 60.54 r - 4.04 V_c \cdot f - 1.02 V_c \cdot ap + 0.25 V_c \cdot r - 931.11 f \cdot ap + 471.39 f \cdot r + 155 ap \cdot r - 0.0025 V_c^2 - 5121.53 f^2 - 333.83 ap^2 - 22.78 r^2 \quad (5)$$

The coefficients values of determination R^2 for the components models of the cutting force F_a , F_r and F_t are respectively $R^2=0.9709$, $R^2=0.994$ and $R^2=0.9954$. These values indicate that 97.09%, 99.4% and 99.54% of the cutting forces variations (F_a , F_r and F_t) are explained by these developed models. The determination coefficients

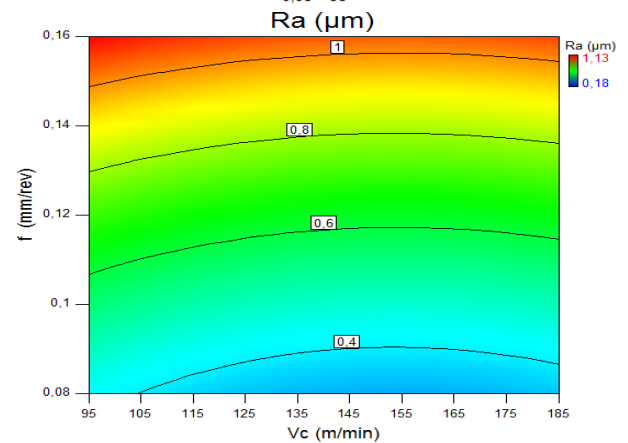
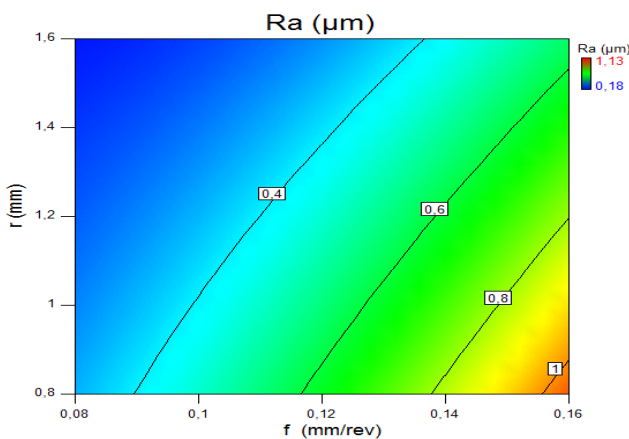
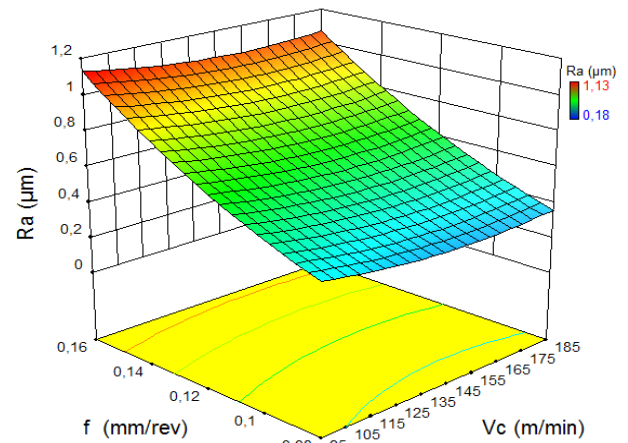
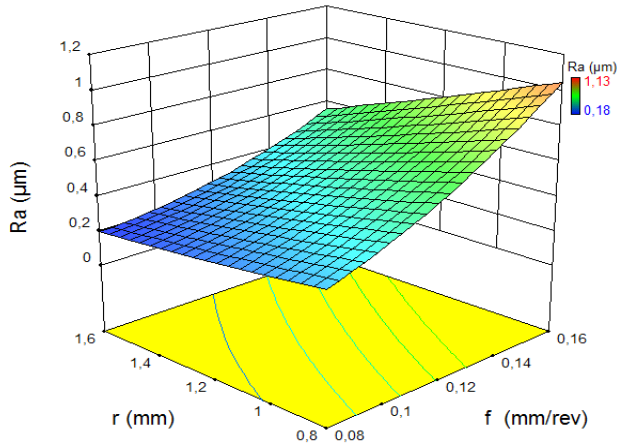


Fig. 8 The feed and tool nose radius effect on the surface roughness (Ra) with ($V_c=140$ m/min, $a_p=0.3$ mm)

Fig. 9 Feed and cutting speed effect on the surface roughness (Ra) with ($r=0.8$ mm, $a_p=0.3$ mm)

values are high suggesting a high significance of the models and show good agreement with the experimental data. Figs. 7(a), (b) and (c) show a comparison between the estimated values of the cutting forces (F_a , F_r and F_t) by the equations of the developed models and the experimental values.

4.5 Response surfaces

A graphical analysis was carried out using Design Expert Software. The surface plots obtained for the most influential factors related to the surface roughness (Ra) and cutting forces (F_a , F_r and F_t) in hard turning with respect to the machining parameters is presented. Figs. 8-13 show the variation of surface roughness and cutting forces with the machining parameters namely cutting speed, feed, and tool nose radius. Fig. 8 shows the variation in the surface roughness with the tool radius nose and feed. It is seen that feed has most significant effect on the surface roughness and its variation is very high when compared with the tool radius nose. The value of the surface roughness (Ra) decreases with the increase of the tool radius nose. Fig.9 shows the surface roughness variation (Ra) with feed and cutting speed. It can be noted that the feed has a more significant impact on the surface roughness. The surface roughness does not change much with the cutting speed for the very high feed range, but tends to decrease almost with the increase of cutting speed at low feed. As has been stated

previously, this figure clearly shows that a low surface roughness can be obtained for any cutting speed (95-185 m/min), but with a very low feed (0.08 mm/rev).

Fig. 10 shows the variation of the surface roughness with the cutting speed and the tool nose radius. It can be noted that the tool nose radius has a significant effect on the surface roughness. As previously pointed out; with the increase of the tool nose radius (close to 1.6 mm), the surface quality becomes better. This happens for a lower feed rate and a higher speed. The surface roughness values (Ra) remain almost constant with the increase in cutting speed and when the tool nose radius varies from 1.2 to 1.6 mm. In general, the surface roughness improves with the increase of the cutting speed.

The variation of the axial force (F_a) with the depth of cut and the cutting speed is shown in Fig. 11, where it is confirmed that the depth of cut has a very significant effect on the axial force (F_a). The axial force (F_a) does not change much as a function of the increase in the cutting speed in particular for the minimum depth of cut (0.15 mm). Fig. 12 shows the estimated response of the radial force (F_r) as a function of feed and the depth of cut. The analysis of this figure shows that the depth of cut has a significant effect on the radial force (F_r). It can also be noted that at the lowest values of the depth of cut, the radial force decreases for any feed level. Fig. 13 shows the variation of the tangential cutting force (F_t) with the depth

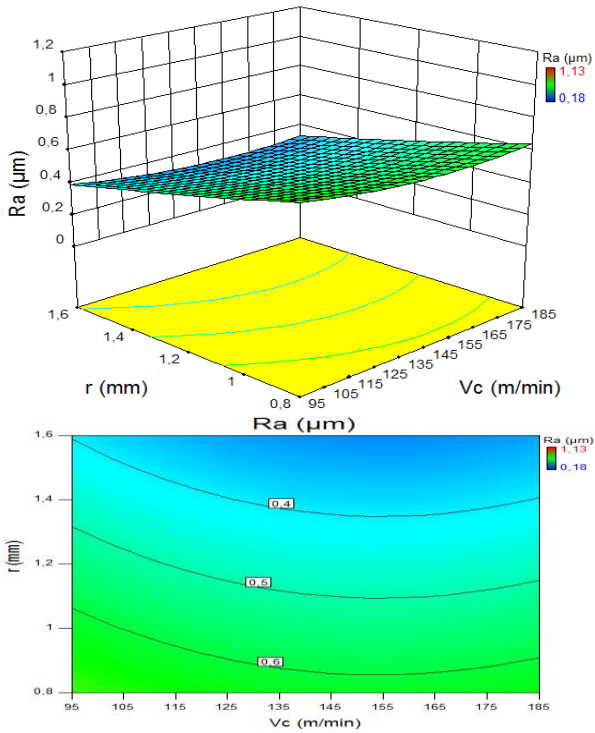


Fig. 10 Effect of cutting speed and tool nose radius on surface roughness with ($f=0.12$ mm/rev, $a_p=0.3$ mm)

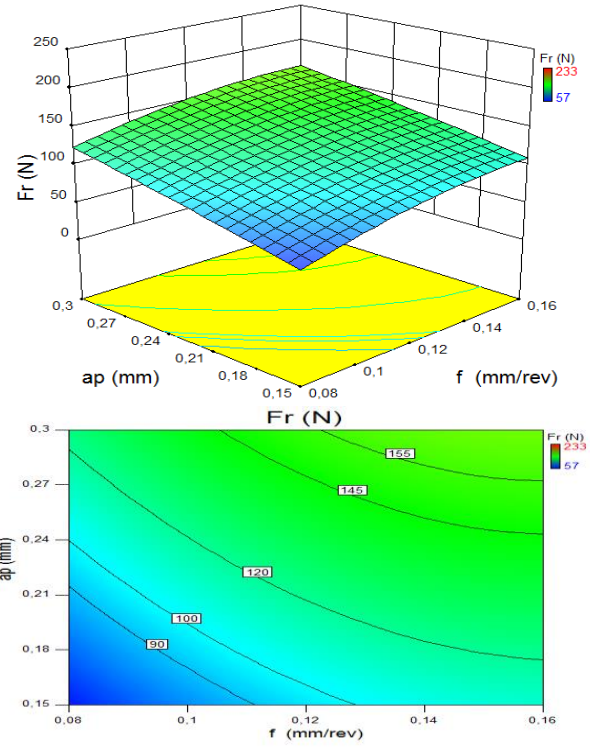


Fig. 12 Effect of feed rate and depth of cut on axial force (Fr) with ($V_c=140$ m/min, $r=1.2$ mm)

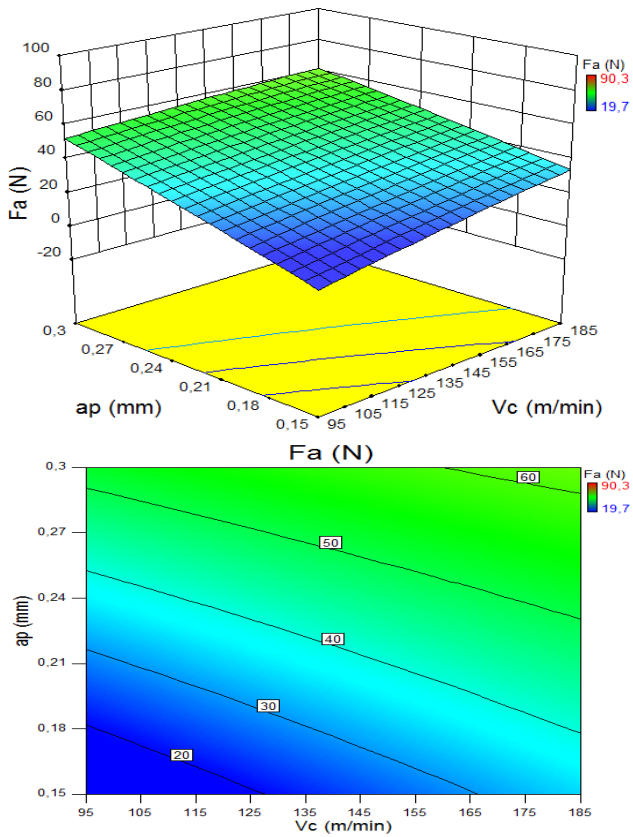


Fig. 11 Effect of cutting speed and depth of cut on the axial force (F_a) with ($f=0.16$ mm/rev, $r=0.8$ mm)

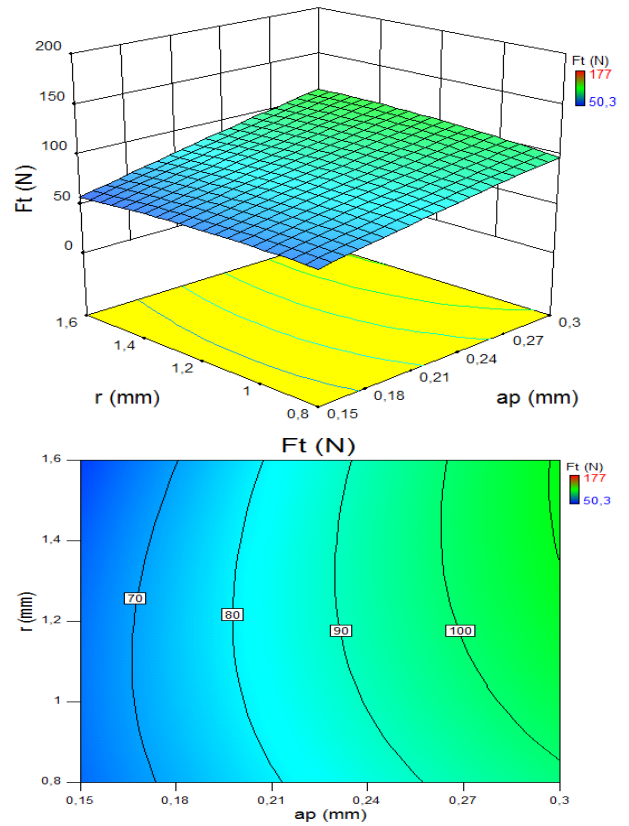


Fig. 13 Effect of depth of cut and tool nose radius on the tangential force (F_t) ($V_c=185$ m/min, $r=0.8$ mm)

of cut and the tool nose radius. For very high feed values and depth of cut, the tangential force is considerably high.

In addition, the depth of cut is the most significant factor on the tangential force (F_t), followed by the tool nose radius.

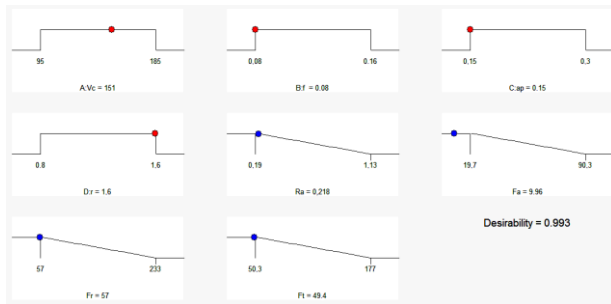


Fig. 14 Multiple response optimization graph of surface roughness (Ra) and cutting forces (Fa , Fr and Ft)

5. Optimization of cutting conditions

At this stage of the work, it is intended to investigate the optimal cutting conditions. The simultaneous optimization technique of several responses of a system is the desirability function. The objective function of this optimization is to the simultaneous minimization of several responses (Ra , Fa , Fr and Ft) illustrated by the system detailed in the reference (Hessainia *et al.* 2013a). Therefore, this study will allow to determine the optimal cutting conditions according to the importance of the user-defined selection criteria between the surface roughness and the cutting forces in order to improve the quality of the machined parts during hard turning bearing steel (AISI 52100) with mixed ceramic tool (CC650). The constraints used during the optimization process are illustrated in Table 9.

The optimal solutions for each studied tool nose radius are given in Table 10 in descending order of desirability. The desirability value 0.993 corresponds to the best value of the surface roughness with minimal cutting forces in the indicated parameters range. By maximizing the desirability function (D) which is the objective function under the constraints of the variables. The following table shows the optimum settings for the cutting conditions for each tool nose radius.

6. Conclusions

In this paper, the response surface methodology (RSM) has been used to study and analyze machining parameters and their interactions which have a statically significant effect during the hard turning of rolling steel (AISI 52100) with a mixed ceramic tool (CC650). Multiple nonlinear regression models are associated with desirability optimization function. The main objective of this study has been to determine the optimum cutting conditions for each nose radius of the tool being studied. The conclusions drawn from this study are:

- The feed rate (f), the tool nose radius (r), the cutting speed (Vc) and the interaction of the feed rate and the tool nose radius ($f \times r$) and the quadratic effect (f^2) all have a significant effect on surface roughness (Ra). Feed rate is the most influential factor with a contribution of 47.31%.

- The axial force (Fa), radial (Fr) and tangential (Ft) are strongly influenced by the depth of cut. Its effect is characterized by a respective contribution of 25.28%,

24.82% and 27.97%. On the other hand, the cutting speed has a very low influence (1.26%) for Fa and not significant for Fr and Ft .

- The best surface quality was obtained for the low feed rate values and the highest values of the tool nose radius.

- The prediction models deduced for the components of the cutting force and the surface roughness are in very good agreement with the values obtained experimentally.

- The optimum conditions for the roughness and the components of the cutting force have been defined for different values of the tool nose radius.

Acknowledgments

This work was achieved in the Advanced Technologies in Mechanical Production Research Laboratory (LRTAPM), Badji Mokhtar-Annaba University, Algeria in collaboration with the Mechanics and Structures Research Laboratory (LMS), May 8th 1945 University, Guelma, Algeria.

The authors would like to thank the Algerian Ministry of Higher Education and Scientific Research (MESRS) and the Delegated Ministry for Scientific Research (MDRS) for granting financial support for CNEPRU Research Project-LRTAPM: A11N01UN230120130011 (Badji Mokhtar-Annaba University).

References

- Aouici, H., Bouchelaghem, H., Yallese M.A., Elbah, M. and Fnides, B. (2014), "Machinability investigation in hard turning of AISI D3 cold work steel with ceramic tool using response surface methodology", *Int. J. Adv. Manuf. Technol.*, **73**(9-12), 1775-1788.
- Asian, E., Camuscu, N. and Birgoren, B. (2007), "Design optimization of cutting parameters when turning hardened AISI 4140 steel (63 HRC) with Al_2O_3/TiC mixed ceramic tool", *J. Mater. Des.*, **28**(5), 1618-1622.
- Azizi, M.W., Belhadi, S., Yallese, M.A., Mabrouki, T. and Rigal, J.F. (2012), "Surface roughness and cutting forces modeling for optimization of machining condition in finish hard turning of AISI 52100 steel", *J. Mech. Sci. Technol.*, **26**(12), 4105-4114.
- Bensouilah, H., Aouici, H., Meddour, I., Yallese, M.A., Mabrouki, T. and Girardin, F. (2016), "Performance of coated and uncoated mixed ceramic tools in hard turning process", *Measure.*, **82**, 1-18.
- Bouacha, K., Yallese, M.A., Khamel, S. and Belhadi, S. (2014), "Analysis and optimization of hard turning operation using cubic boron nitride tool", *Int. J. Refr. Met. Har. Mater.*, **45**, 160-178.
- Bouacha, K., Yallese, M.A., Mabrouki, T. and Rigal, J.F. (2010), "Statistical analysis of surface roughness and cutting forces using response surface methodology in hard turning of AISI 52100 bearing steel with CBN tool", *J. Refract. Met. Hard. Mater.*, **28**(3), 349-361.
- Bouaid, L., Yallese, M.A. and Belhadi, S., (2014), "RMS-based optimisation of surface roughness when turning AISI 420 stainless steel", *Int. J. Mater. Prod. Technol.*, **49**(4), 224-251.
- Das, D.K., Panda, A. and Dhupal, D. (2017), "Analysis of surface roughness in hard turning with coated ceramic inserts: Cutting parameters effects, prediction model, cutting conditions optimization and cost analysis" *Ciën.e Técn.Vitivin.*, **32**(1) 127-154.

- Gunay, M. and Yucel, E. (2013), "Application of Taguchi method for determining optimum surface roughness in turning of high-alloy white cast iron", *Measure.*, **46**(2), 913-919.
- Hessainia, Z., Belbah, A., Yallese, M.A. and Mabrouki, R. (2013), "On the prediction of surface roughness in the hard turning based on cutting parameters and tool vibrations", *Measure.*, **46**(5), 1671-1681.
- Hessainia, Z., Kribes, N., Yalles, M.A., Mabrouki, T., Ouclaa, N. and Rigal, J.F. (2013), "Turning roughness model based on tool-nose displacements", *Mech.*, **19**(1), 112-119.
- Kablouti, O., Boulanouar, L., Azizi, M.W. and Yallese, M.A. (2017), "Effects of coating material and cutting parameters on the surface roughness and cutting forces in dry turning of AISI 52100 steel", *Struct. Eng. Mech.*, **61**(4), 519-526.
- Kevin Chou, Y. and Hui, S. (2004), "Tool nose radius effects on finish hard turning", *J. Mater. Proc. Technol.*, **148**(2), 259-268.
- Kumar, A.S., Durai, A.R. and Sornakumar, T. (2003), "Machinability of hardened steel using alumina based ceramic cutting tools", *Int. J. Refract. Met. Hard. Mater.*, **21**(3-4), 109-117.
- Meddour, I., Yallese, M.A., Khattabi, R., Elbah, M. and Boulanouar, L. (2015), "Investigation and modeling of cutting forces and surface roughness when hard turning of AISI 52100 steel with mixed ceramic tool: Cutting conditions optimization", *Int. J. Adv. Manufact. Technol.*, **77**(5-8), 1387-1399.
- Montgomery, D.C. (2001), *Design and Analysis of Experiments*, 5th Edition, John Wiley & Sons Inc, New York, U.S.A.
- Neşeli, S., Yıldız, S. and Türkes, E. (2011), "Optimization of tool geometry parameters for turning operations based on the response surface methodology", *Measure.*, **44**(3), 580-587.
- Özel, T. and Kapat, Y. (2005), "Predictive modeling of surface roughness and tool wear in hard turning using regression and neural networks", *Int. J. Adv. Manufact. Technol.*, **45**(4-5), 467-479.
- Paiva, A.P., Campos, P.H., Ferreira, J.R., Lopes, L.G.D., Paiva, E.J. and Balestrassi, P.P. (2012), "A multivariate robust parameter design approach for optimization of AISI 52100 hardened steel turning with wiper mixed ceramic tool", *J. Refract. Met. Hard. Mater.*, **30**(1), 152-163.
- Paiva, A.P., Paiva, E.J., Ferreira, J.R., Balestrassi, P.P. and Costa, S.C. (2009), "A multivariate mean square error optimization of AISI 52100 hardened steel turning", *Int. J. Adv. Manufact. Technol.*, **43**(7-8), 631-643.
- Rashid, W.B., Goel, S., Davim, J.P. and Joshi, S.N. (2016), "Parametric design optimization of hard turning of AISI 4340 steel (69 HRC)", *Int. J. Adv. Manufact. Technol.*, **82**(1), 451-462.
- Shihab, S.K., Khan, Z.A., Mohammad, A. and Siddiquee, A.N. (2014), "Optimization of surface integrity in dry hard turning using RSM", *Sadh.*, **39**(5), 1035-1053.
- Xiaobin, C., Jingxia Guo, G. and Jianxin, Z. (2016), "Optimization of geometry parameters for ceramic cutting tools in intermittent turning of hardened steel", *Mater. Des.*, **92**, 424-437.
- Yallese, M.A., Chaoui, K., Zeghib, N., Boulanouar, L. and Rigal, J.F. (2009), "Hard machining of hardened bearing steel using cubic boron nitride tool", *J. Mater. Pr. Technol.*, **209**(2), 1092-1104.
- Yin, Z., Huang, C., Yuan, J., Zou, B., Liu, H. and Zhu, H. (2015), "Cutting performance and life prediction of an Al₂O₃/TiC micro-nano-composite ceramic tool when machining austenitic stainless steel", *Ceram. Int.*, **41**(5), 7059-7065.